ChemComm

Chemical Communications

Accepted Manuscript

Volume 54
Number 1
4 January 2018
Pages 1-112

ChemComm

Chemical Communications

rsc.li/chemcomm

ISSN 1359-7345

COMMUNICATION
S. J. Connon, M. O. Senge et al.
Conformational control of nonplanar free base porphyrins:
towards bifunctional catalysts of tunable basicity

ROYAL SOCIETY
OF CHEMISTRY

rsc.li/chemcomm

COMMUNICATION

Hydrosilylation of B≡B Triple Bonds: Catalyst- and Reductant-Free Construction of B–Si bonds and B₂Si Heterocycles

Tobias Brückner,[a,b] Dario Duwe,[a,b] Felipe Fantuzzi,[a,b,c,d] Merlin Heß,[a,b] Rian D. Dewhurst,[a,b] Krzysztof Radacki,[a,b] Holger Braunschweig[a,b]*

Hydrosilanes undergo mild, uncatalyzed single and double 1,2-addition across the B–B triple bonds of diborynes, leading to an unsymmetrical silyldiborene and compounds with novel non-cluster three-membered B₂Si rings. The reactions are a new addition to the very few catalyst- and alkali-metal-free methods available for the construction of B–Si bonds.

Borylsilanes, $R_2B–SiR'_3$, are relatively reactive compounds that are most well known for their use in silaboration reactions of unsaturated compounds, usually requiring a catalyst. This reaction has the enticing advantage that it installs two functionalizable – but different – groups (i.e. boryl BR_2 and silyl SiR'_3) at adjacent carbon atoms, allowing sequential derivatization at these points. Consequently, this protocol has attracted wide interest from organic chemistry, and advances in the reaction have frequently been reviewed.[1]

The construction of B–Si bonds is often non-trivial, due to a general lack of nucleophilic reagents based on either boron or silicon. This is most frequently accomplished by: (a) nucleophilic attack of an alkali metal silyl species at a haloborane,[1e,2] (b) nucleophilic attack of an anionic boron species at a halo- or alkoxysilane,[3] (c) reactions of a silylene [R_2Si:] with a tricoordinate boron species via either adduct formation or B–X bond insertion,[4] and hydroboration of disilenes.[5] In contrast, B–Si bond construction without an alkali-metal nucleophile or a silylene is limited to just a handful of isolated examples, for instance a silyl ligand migration to boron on a tantalum scaffold and an iridium-catalyzed hydrosilylation of a diborene.[6]

The development of reactive doubly Lewis-base-stabilized molecules containing B–B multiple bonds[7] has led to the discovery of a range of novel intermolecular bond activation reactions, resulting in 1,2-addition across the B–B bonds. Doubly base-stabilized diborynes [LB≡BL] (L = Lewis base such as NHC or CAAC), have shown the propensity to activate the H–H bond of dihydrogen,[8] the C–O bonds of CO and CO_2,[9,10] B–H[11] and B–B[12] bonds, S–S and Se–Se bonds,[13] and even the activated C–H bonds of acetone and alkynes.[14,15] This reactivity accordingly led us to attempt the hydrosilylation of a diboryne,

a process that would be the conceptual inverse of Sekiguchi's hydroboration of disilynes (RSi≡SiR).[5] Herein we describe the first examples of single and double hydrosilylation of a B≡B triple bond, under mild conditions and without a catalyst, leading to an unsymmetrical silyldiborene and highly unusual compounds with three-membered B₂Si rings. The results are a new entry to B–Si bond construction, and one of only a few that occur without the need for alkali metal reagents or silylene precursors.
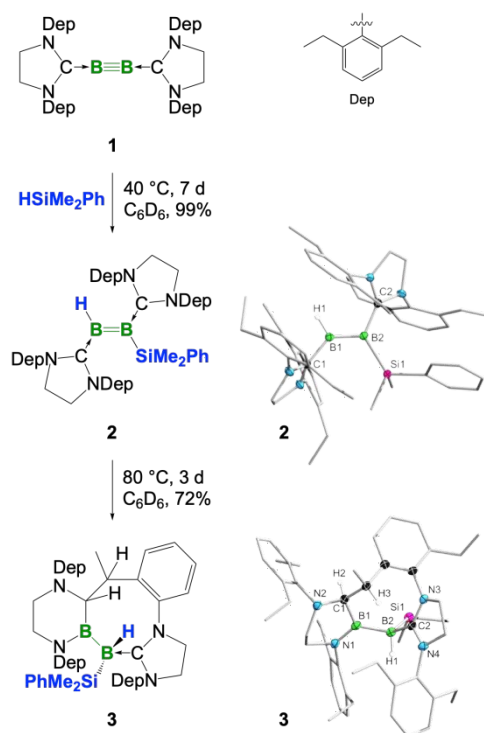
Fig. 1 Left: Single Si–H activation and thermal rearrangement. Stereochemistry shown is relative only. Right: Crystallographically-derived structures of **2** and **3**. Ellipsoids shown at the 50% probability level. Ellipsoids of peripheral groups, most hydrogen atoms, the phenyl substituent of the silicon atom in **3**, and all solvent molecules have been removed for clarity.

The doubly *N*-heterocyclic-carbene-stabilized diboryne [(SIDep)B≡B(SIDep)] (**1**, SIDep = 1,3-bis(2,6-diethylphenyl)-imidazolin-2-ylidene; Figure 1, top) has thus far shown the highest reactivity of all of the known species of the form LB≡BL[7-15] and was therefore chosen for use in initial reactivity tests with hydrosilanes. Treatment of **1** with an equimolar amount (or an excess) of dimethyl(phenyl)silane in C_6D_6 led to a color change from red to pink overnight, but with only minimal conversion

a. *Institute for Inorganic Chemistry, Julius-Maximilians-Universität Würzburg, Am Hubland, 97074 Würzburg, Germany.*

b. *Institute for Sustainable Chemistry & Catalysis with Boron, Julius-Maximilians-Universität Würzburg, Am Hubland, 97074 Würzburg, Germany.*

c. *Institute for Physical and Theoretical Chemistry, Julius-Maximilians-Universität Würzburg, Emil-Fischer-Straße 42, 97074 Würzburg (Germany)*

d. *School of Chemistry and Forensic Science, University of Kent, Park Wood Rd, Canterbury CT2 7NH (UK)*

ARTICLE

according to ^{11}B (**1**: $\delta(^{11}$B) = 56 ppm) and ^{1}H NMR spectroscopic monitoring. After heating the mixture to 40 °C for one week, a new set of ^{11}B NMR signals was observed at 35 and 21 ppm, in addition to ^{1}H NMR signals corresponding to an unsymmetrical diborene. These data suggested the clean, near-quantitative conversion to 1-hydro-2-silyldiborene **2**. After evaporation of all volatiles under high vacuum, the red solid **2** was isolated in 99% yield (Figure 1, middle). The ^{1}H NMR spectrum shows two singlets at 3.17 and 3.08 ppm corresponding to the carbene backbone protons and superimposed multiplets ($\delta(^1$H) = 2.78-2.45 ppm) for the ethyl groups, as well as a singlet at $\delta(^1$H) = −0.11 ppm representing the silicon-bound methyl groups. The ^{11}B-decoupled ^{1}H NMR spectrum shows an intensified signal at 4.48 ppm, which can be assigned to the boron-bound hydrogen atom. Signals for the carbene carbon atoms were found as broad resonances in the ^{13}C{^{1}H} NMR spectrum at $\delta(^{13}$C) = 194.1 and 191.6 ppm, while a signal was detected in the ^{29}Si NMR spectrum at $\delta(^{29}$Si) = 18.9 ppm. During the heating process, no further color change occurs, reflecting the intense color of **2**. Diborene **2** shows an absorption maximum at λ = 570 nm as well as a second band at λ = 420 nm in its UV/vis spectrum (see Supporting Information).

A single-crystal X-ray diffraction (SCXRD) study unequivocally revealed **2** to be the expected diborene.[16] The solid-state structure of diborene **2** (Figure 1, middle) shows a B1–B2 distance of 1.609(2) Å, lying in the typical range for doubly NHC-stabilized diborenes.[8,17] The slightly differing B–C^{NHC} distances of 1.574(2) (C1–B2) and 1.544(2) Å (B2–C2), respectively, suggest different degrees of π-donation from the electron-rich B$_2$ unit to the carbene. This is also evident from the alignment of the NCN planes of the ligands with the B=B bond. The ligand of the shorter B2–C2 bond is tilted with respect to the B–B double bond by ca. 27°, while the deflection of the second NHC is ca. 54°. The B2–Si1 distance (2.008(2) Å) is relatively short compared to typical B-Si single bonds.[18]

For a more in-depth examination of the electronic structure and bonding situation of **2**, we conducted DFT calculations on this compound. Figure 2A shows the frontier Kohn–Sham molecular orbitals (MOs) of **2**. As expected, both the HOMO and LUMO are consistent with typical diborenes. The HOMO exhibits a (B–B)π contribution, characterized by an in-phase combination of the boron p$_z$ orbitals. Conversely, the LUMO features a nodal plane in the B–B region, thus representing the out-of-phase combination of the boron p$_z$ orbitals. To gain deeper insights into the π-donation from the B$_2$ motif to the carbenes, we performed intrinsic bond orbital (IBO)[19] calculations, as illustrated in Figure 2B. Analysis of the electron distribution within the IBO associated to the B–B π bond reveals significant disparities in the contributions of the carbene centers. Specifically, C1 contributes to a mere 3.50% to the IBO, while the contribution of C2 is approximately five times more pronounced (18.0%). These findings align with the above speculations based on the solid-state structure and confirm that π donation to the carbene centers is uneven, a consequence of the varying tilting angles of the carbenes relative to the CBBC plane, which in turn likely originates from steric effects.

Preliminary experiments showed that heating mixtures of dimethyl(phenyl)silane and **1** above 40 °C provided a signal in the four-coordinate region of the ^{11}B NMR spectrum (−34 ppm). This prompted us to heat an isolated sample of **2** for three days in benzene to 80 °C (Figure 1), leading to selective generation of the same signal observed starting from **1**. After removal of the solvent, washing with hexamethyldisiloxane, and recrystallization from hexane, the rearrangement product **3** was isolated as a colorless crystalline solid in 72% yield. A SCXRD study identified **3** as an unusual azadiboracyclooctene derivative (Figure 1, right bottom). Two signals are detected in the ^{11}B NMR spectrum of **3** at $\delta(^{11}$B) = 56 and −34 ppm. In accordance with the asymmetry of the system, but in contrast to **2**, the ^{1}H{^{11}B} NMR spectrum shows two signals for the Si-CH$_3$ protons at $\delta(^1$H) = 0.08 and 0.29 ppm, as well as partially overlapping multiplets for the ethyl groups and the CH$_2$ backbone atoms ($\delta(^1$H) = 3.55, 2.10 ppm). The NC(H)B proton can be detected as a doublet ($^3J_{HH}$ = 9.24 Hz) signals $\delta(^1$H) = 3.97 ppm and the CHCH$_3$ atom as a multiplet at $\delta(^1$H) = 3.74 ppm. The corresponding carbon atoms are found in the carbon spectrum at $\delta(^{13}$C) = 63.7 and 41.2 ppm, respectively. The boron-bound hydrogen was assigned to a resonance at $\delta(^1$H) = 0.87 ppm. In the ^{13}C{^{1}H} NMR spectrum, a broad resonance at $\delta(^{13}$C) = 203.3 ppm detected by 2D-^{13}C,^{1}H-HMBC experiments can be assigned to the carbene carbon atom. The CH$_2$ backbone atoms are detected as four signals between $\delta(^{13}$C) = 56.3 and 51.2 ppm. Although **3** contains three stereocenters, the NMR data suggest that only one diastereomer is formed during the rearrangement. The solid-state structure of **3** is shown in Figure 1. The B–B distance of 1.740(3) Å is in line with known sp^2-sp^3 diboranes.[20] Our calculations reflect the relative inertness of **3** relative to **2**, in particular the significantly larger HOMO-LUMO gap of **3** (4.90 eV), which is 1.84 eV greater than that of **2**. Furthermore, free energy calculations for both systems reveal that **3** exhibits remarkable stability compared to **2**, with the transformation of **2** to **3** being exergonic by −46.4 kcal mol^{-1}.

In contrast to the reactions of diborynes with HBcat, which result in twofold B–H addition and tetraborane products,[11] only single addition takes place with the tertiary silane HSiMe$_2$Ph. This prompted us to test the reaction of **1** with phenylsilane (H$_3$SiPh, Figure 3). This reaction produced a color change from red to pink within two hours, suggesting formation of the corresponding diborene, and ultimately to yellow after an additional three hours, suggesting consumption of the diborene. ^{11}B ($\delta(^{11}$B) = −29, −33 ppm) and ^{1}H{^{11}B} NMR spectra ($\delta(^1$H) = −0.15 (m), 0.37 (m) ppm) of the reaction mixture suggested that double Si-H activation had taken place. A colorless solid corresponding to a single addition of H$_3$SiPh to **1** was obtained in 83% yield, which we assumed to be the compound **4**, with a B$_2$Si central ring. The two similar ^{11}B NMR signals detected suggest either the presence of *rac* (*trans* at B–B) and *meso* (*cis* at B–B) diastereomers, or that the two boron nuclei are made inequivalent by different and locked ligation geometries of the NHC units. The latter case seemed far more likely, as (a) a *cis* geometry with respect to the B–B bond would be exceptionally crowded, and (b) the ^{29}Si{^{1}H} NMR spectrum

shows a single, sharp singlet ($\delta(^{29}Si)$ = 28.5 ppm), while the *rac/meso* situation would likely lead to two signals.
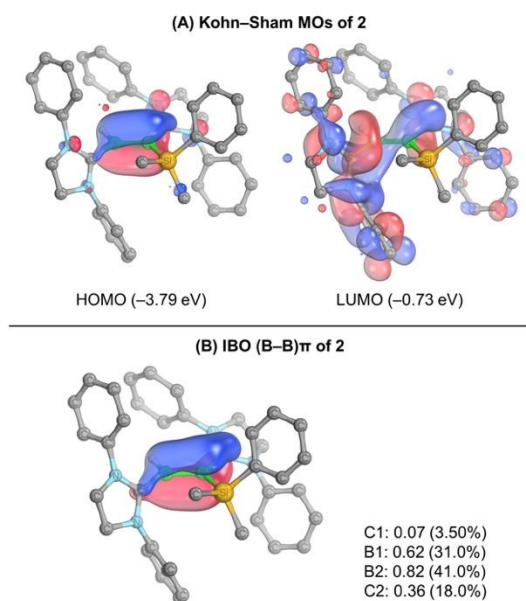

Fig. 2 (A) Kohn–Sham MOs of **2**. A HOMO-LUMO gap of 3.06 eV is obtained for 2 at the PBE0/def2-SVP level. (B) Intrinsic bond orbital (IBO) of **2** depicting its B–B π bond. Numbers indicate the proportion of electrons from the doubly occupied IBO assigned to each individual atom, along with their corresponding percentages. Atom numbering is as shown in Figure 1, middle. To enhance clarity, hydrogen atoms except H1 and the ethyl groups at the NHC periphery have been excluded from all orbital plots. Isosurfaces have been constructed to enclose 70% of the electron density.

Single crystals of **4** suitable for SCXRD analysis were obtained by evaporation of a saturated hexane solution. The resulting solid-state structure is shown in Figure 3, confirming the double Si–H addition across the B–B triple bond and formation of a B$_2$Si ring. However, contrary to our assumptions about the ^{11}B{^{1}H} NMR spectrum, the ligation geometries of the NHC units in this structure are very similar, which is likely due to a difference in the solution and solid-state structures of the compound. The B1–B2 distance of 1.732(2) Å) is within the typical range for diboranes, and the boron–silicon bond lengths (2.007(3) and 2.008(3) Å) are also within the expected single-bond range.[21] To the best of our knowledge, siladiborirane **4** represents the first example of a non-cluster compound containing a B$_2$Si ring.

In an attempt to extend this double hydrosilylation concept to a bis(silyl) precursor, combination of two equivalents of **1** with one equivalent of 1,4-disilylbenzene in benzene gave an orange crystalline solid formed directly in the reaction solution with ^{11}B{^{1}H} NMR signals at –29 and –33 ppm, a single ^{29}Si{^{1}H} NMR signal at –25.9 ppm, and a single ^{1}H NMR signal for the Si–H nuclei at 3.38 ppm, suggesting the formation of bis(siladiborirane) **5** (Figure 3). After washing with benzene, **5** was isolated in 74% yield. Although more stereochemical possibilities are possible in the assumed bis(diborane) product **5**, the striking similarity of the ^{11}B and ^{29}Si NMR spectroscopic data suggests that, like in **4**, the two ^{11}B NMR signals are due to different ligation geometries of the NHC units. The solid-state structure of **5** is shown in Figure 3. Like the NMR spectra, the

geometries of the B$_2$Si units of **5** are comparable to those of **4**. A notable feature of the structure is the parallel arrangement of the B$_2$Si planes in **5**, which are tilted ca. 66° with respect to the bridging phenyl ring. In contrast to the colorless **4**, **5** is orange in both the solid state and solution, in line with its UV/vis spectrum, which shows broad absorptions covering the violet-to-green range (λ_{max} = 352 nm with a weaker band at λ = 470 nm; see SI).
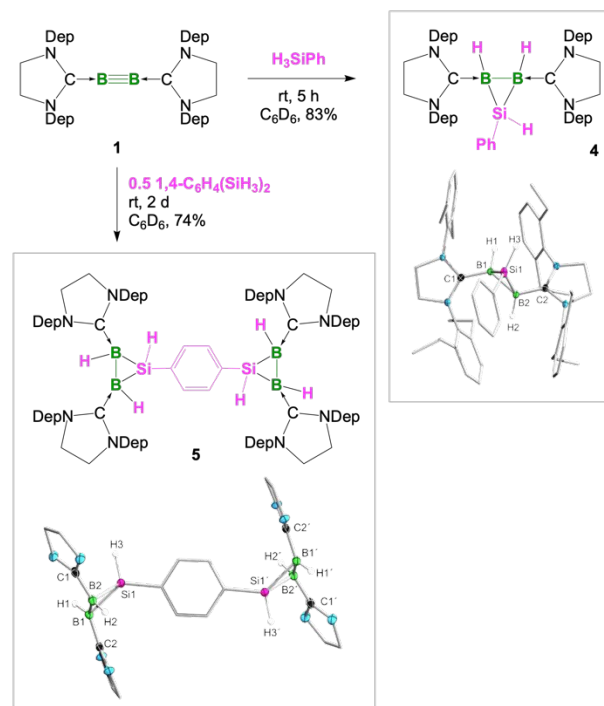
Fig. 3 Top: Double Si–H activation to form **4** and **5**. Bottom: Crystallographically-derived structures of **4** (left) and **5** (right). Ellipsoids shown at the 50% probability level. Ellipsoids of peripheral groups, Dep substituents of **5**, most hydrogen atoms, and all solvent molecules have been removed for clarity.
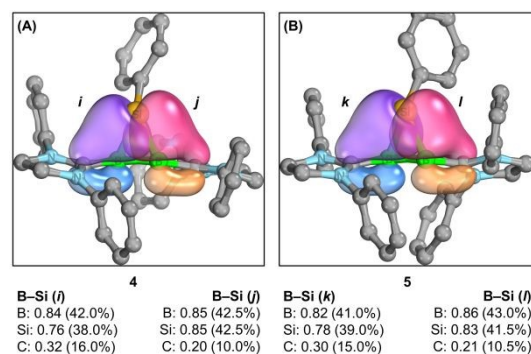
Fig. 4 Selected IBOs of (A) **4** and (B) **5**. Hydrogen atoms are omitted for clarity. Numbers indicate the proportion of electrons from the doubly occupied IBO assigned to each individual atom, along with their corresponding percentages. Ethyl groups at the NHC periphery omitted for clarity.

To gain further insight into the bonding situation within these unique B$_2$Si rings, we carried out IBO calculations on **4** and **5** (Figure 4). As expected, our findings clearly indicate the absence of π bonding between the boron centers. However, a closer examination of the IBOs associated with the B–Si σ bonds

reveals a non-negligible degree of donation to the carbenes. Indeed, carbon centers contribute to these orbitals in the range of 10-16%. This donation from the B–Si σ bonds to the vacant p orbitals at the NHC carbon atoms is likely an example of a form of hyperconjugation known as the β-silicon effect,[22] similar to that observed by Siehl et al. in a β-silyl-substituted vinyl cation.[23] Similar to the diborene, these donations exhibit uneven distribution, stemming from distinct tilting angles arising from unequal steric effects.

We present herein the first hydrosilylation reactions of B–B multiple bonds, both single (with a tertiary silane) and double (with primary silanes). The single hydrosilylation leads to formation of a rare example of an unsymmetrical diborene, while the double hydrosilylation reactions produce novel mono- and bis(siladiboriranes) containing B_2Si rings.

Conflicts of interest

There are no conflicts to declare.

Notes and references

1   (a) M. Suginome and Y. Ito, *J. Organomet. Chem.*, 2003, **680**, 43–50; (b) H. E. Burks and J. P. Morken, *Chem. Commun.,* 2007, 4717–4725; (c) T. Ohmura and M. Suginome, *Bull. Chem. Soc. Jpn.,* 2009, **82**, 29–49; (d) M. Suginome and T. Ohmura, *Transition Metal-Catalyzed Element-Boryl Additions to Unsaturated Organic Compounds*, in *Boronic Acids: Preparation and Applications in Organic Synthesis, Medicine and Materials*. Ed. D. G. Hall, Wiley-VCH Verlag GmbH & Co. KGaA, 2011, pp 171–212; (e) M. Oestreich, E. Hartmann and M. Mewald, *Chem. Rev.,* 2013, **113**, 402–441; (f) P. K. Verma, M. L. Shegavi, S. K. Bose and K. Geetharani, *Org. Biomol. Chem.,* 2018, **16**, 857–873; (g) M. Stratakis and I. N. Lykakis, *Synthesis,* 2019, **51**, 2435–2454; (h) C. Moberg, *Synthesis,* 2020, **52**, 3129–3139.

2   (a) S. Inoue, I. Masaaki and A. Sekiguchi, *Chem. Lett.,* 2008, **37**, 1044–1045; (b) P. Willmes, K. Leszczyńska, Y. Heider, K. Abersfelder, M. Zimmer, V. Huch and D. Scheschkewitz, *Angew. Chem. Int. Ed.* 2016, **55**, 2907; (c) T. Kosai and T. Iwamoto, *J. Am. Chem. Soc.*, 2017, **139**, 18146; (d) Y. Heider, P. Willmes, V. Huch, M. Zimmer and D. Scheschkewitz, *J. Am. Chem. Soc.*, 2019, **141**, 19498; (e) K. Tanaka, N. Akasaka, T. Kosai, S. Honda, Y. Ushijima, S. Ishida and T. Iwamoto, *Molecules*, 2021, **26**, 1632.

3   (a) A. V. Protchenko, K. H. Birjkumar, D. Dange, A. D. Schwarz, D. Vidovic, C. Jones, N. Kaltsoyannis, P. Mountford and S. Aldridge, *J. Am. Chem. Soc.,* 2012, **134**, 6500–6503; (b) M. Arrowsmith, D. Auerhammer, R. Bertermann, H. Braunschweig, M. A. Celik, J. Erdmannsdörfer, I. Krummenacher and T. Kupfer, *Angew. Chem. Int. Ed.,* 2017, **56**, 11263–11267; (c) Z. Liu and C. Cui, *J. Organomet. Chem.,* 2020, **906**, 121041; (d) J. Gilmer, M. Bolte, A. Virovets, H.-W. Lerner, F. Fantuzzi and M. Wagner, *Chem. Eur. J.,* 2023, **29**, e202203119; (e) J. Gilmer, T. Trageser, L. Čaić, A. Virovets, M. Bolte,

H.-W. Lerner, F. Fantuzzi and M. Wagner, *Chem. Sci.,* 2023, **14**, 4589–4596.

4   See, for example: (a) A. Rosas-Sánchez, I. Alvarado-Beltran, A. Baceiredo, D. Hashizume, N. Saffon-Merceron, V. Branchadell and T. Kato, *Angew. Chem. Int. Ed.,* 2017, **56**, 4814–4818; (b) H. Wang, L. Wu, Z. Lin and Z. Xie, *J. Am. Chem. Soc.,* 2017, **139**, 13680–13683.

5   (a) K. Takeuchi, M. Ikoshi, M. Ichinohe, A. Sekiguchi, *J. Am. Chem. Soc.*, 2010, **132**, 930; (b) K. Takeuchi, M. Ichinohe, A. Sekiguchi, *Organometallics*, 2011, **30**, 2044.

6   (a) Q. Jiang, P J. Carroll and D. H. Berry, *Organometallics* 1993, **12**, 177–183; (b) T. A. Boebel and J. F. Hartwig, *Organometallics,* 2008, **27**, 6013–6019.

7   (a) H. Braunschweig and R. D. Dewhurst, *Angew. Chem. Int. Ed.,* 2013, **52**, 3574-3583; (b) M. Arrowsmith, H. Braunschweig and T. E. Stennett, *Angew. Chem. Int. Ed.,* 2017, **56**, 96-115.

8   M. Arrowsmith, J. Böhnke, H. Braunschweig, M. A. Celik, T. Dellermann and K. Hammond, *Chem. Eur. J.,* 2016, **22**, 17169-17172.

9   M. Arrowsmith, J. Böhnke, H. Braunschweig and M. A. Celik, *Angew. Chem. Int. Ed.,* 2017, **56**, 14287–14292.

10 A. Stoy, J. Böhnke, J.O.C. Jimenéz-Halla, R. D. Dewhurst, T. Thiess and H. Braunschweig, *Angew. Chem. Int. Ed.,* 2018, **57**, 5947–5951.

11 T. Brückner, T. E. Stennett, M. Heß and H. Braunschweig, *J. Am. Chem. Soc.,* 2019, **141**, 14898–14903.

12 T. Brückner, R. D. Dewhurst, T. Dellermann, M. Müller and H. Braunschweig, *Chem. Sci.,* 2019, **10**, 7375–7378.

13 J. Böhnke, T. Dellermann, M. A. Celik, I. Krummenacher, R. D. Dewhurst, S. Demeshko, W. C. Ewing, K. Hammond, M. Heß, E. Bill, E. Welz, M. Röhr, R. Mitrić, B. Engels, F. Meyer and H. Braunschweig, *Nat. Commun.,* 2018, **9**, 1197.

14 J. Böhnke, T. Brückner, A. Hermann, O. F. González-Belman, M. Arrowsmith, J. O. C. Jiménez-Halla and H. Braunschweig, *Chem. Sci.,* 2018, **9**, 5354–5359.

15 T. Brückner, M. Arrowsmith, M. Heß, K. Hammond, M. Müller and H. Braunschweig, *Chem. Commun.,* 2019, **55**, 6700–6703.

16 CCDC deposition numbers 2301095-2301098 contain the supplementary crystallographic data for this paper.

17 Y. Wang, B. Quillian, P. Wei, C. S. Wannere, Y. Xie, R. B. King, H. F. Schaefer, III, P. v. R. Schleyer and G. H. Robinson, *J. Am. Chem. Soc.,* 2007, **129**, 12412–12413.

18 E. Bonnefon, M. Birot, J. Dunogues, J.-P. Pillot, C. Courseille and F. Taulelle, *Main Group Met. Chem.,* 1996, **19**, 761–767.

19 G. Knizia, *J. Chem. Theory Comput.,* 2013, **9**, 4834–4843.

20 H. Braunschweig, A. Damme, R. D. Dewhurst, T. Kramer, T. Kupfer, K. Radacki, E. Siedler, A. Trumpp, K. Wagner and C. Werner, *J. Am. Chem. Soc.,* 2013, **135**, 8702–8707.

21 (a) H. Braunschweig, M. Colling, C. Kollann and U. Englert, *J. Chem. Soc., Dalton Trans.,* 2002, 2289–2296; (b) A. Gackstatter, H. Braunschweig, T. Kupfer, C. Voigt and N. Arnold, *Chem. Eur. J.,* 2016, **22**, 16415–16419.

22 R. Beļaunieks, M. Puriņš and M. Turks, *Synthesis,* 2020, **52**, 2147–2161.

23 H.-U. Siehl, F.-P. Kaufmann, Y. Apeloig, V. Braude, D. Danovich, A. Berndt and N. Stamatis, *Angew. Chem. Int. Ed. Engl.,* 1991, **30**, 1479–1482.